Test of advanced Faddeev calculations and search for three-body force effects in the reaction $^2H(\vec{p},pp)n$ at $E_p = 14.1$ MeV

M. Karus, M. Buballa, J. Helten, B. Laumann, R. Melzer, P. Niessen, H. Oswald, G. Rauprich, J. Schulte-Uebbing, and H. Paetz gen. Schieck
Institut für Kernphysik, Universität Köln, D-5000 Köln, Federal Republic of Germany
(Received 10 September 1984)

Differential cross section and analyzing power of the breakup reaction $^2H(\vec{p},pp)n$ have been measured in a kinematically complete coincidence experiment for two selected kinematical configurations, the final state interaction and the collinear configuration with the neutron at rest in the c.m. system. Faddeev calculations done with a code by Stuivenberg and in particular with a recent code by Doleschall show good agreement with the data. Even in the collinear case which is assumed to be most sensitive to effects of the three-body force, no influence of three-body forces is observed. Their contribution therefore cannot exceed the experimental error of 2–3 %. The results indicate that contributions from P and D waves as well as the tensor force are more important than effects from a three-body force.

I. INTRODUCTION

The three-nucleon system is generally considered an important testing ground for the nucleon-nucleon potential parameters as they are used in three-body Faddeev calculations. It is the simplest system with more than two nucleons and phenomena, such as three-body force and off-shell effects, which would not be observable in the interaction between two nucleons that might appear here. Since many recent Faddeev calculations (see e.g., Refs. 1–3) show good agreement with the differential cross section data, the present experiment was designed to be more sensitive to more sophisticated potential parameter sets by

(1) measuring in a kinematically complete configuration, thus providing the maximum information about the reaction;

(2) measuring the analyzing power in addition to the cross section along the kinematical curve, since polarization observables usually are more sensitive to interference effects;

(2) choosing selected kinematical situations such as the final state interaction (FSI) and the collinear geometry; and

(4) measuring with an experimental accuracy improved over previous experiments.

The existence and manifestation of three-body forces in low-energy nuclear physics has been a long-standing question. The inclusion of a three-body force in calculations of the binding energies of ^{3}He and ^{3}H and also the radius of the triton appeared to improve the results considerably,[4–6] whereas no indication of three-body force effects in scattering experiments has been observed.

The collinear configuration, in which all three particles in the exit channel move collinearly, and especially the collinear situation in which in the c.m. system the neutron is at rest and the two protons are symmetrical with respect to the neutron, has been proposed on more intuitive grounds[7] to be most suited to search for three-body force effects in the $^2H(p,pp)n$ breakup reaction. First calculations of the Bochum group[8,9] confirmed this suggestion by showing that such effects on the breakup cross section are largest for the collinear situation. The predicted size of the effects as compared to the two-body cross section is up to 10% and the effects are distributed over a larger region of the kinematical curve around the exact collinearity point. Therefore, no pronounced and localized effect from three-body forces is to be expected. In the Bochum calculations comparatively simple two-body potentials were used (the Malfliet-Tjon potential with S waves only and the rank-one Yamaguchi form factor). The aim of these calculations was to show the possible influence of three-body forces, and they cannot be expected to give a quantitative comparison with the experimental data. No Faddeev calculations with realistic two-body potentials (e.g., with higher waves and including the tensor force) supplemented by a three-body force exist so far. Neither is there any prediction of three-body force effects on polarization observables.

The present experiment was designed to allow a comparison of the data with two-body Faddeev calculations for two kinematical situations, one of which was the collinear one where three-body force effects would show up most strongly, the other one is the FSI configuration. The FSI dominates the breakup process and therefore yields relatively high cross sections. The p-n FSI is strongest for those points on the kinematical curve for which the relative energy E_{pn} between proton and neutron becomes zero corresponding to a virtual deuteron d* (singlet deuteron). The Bochum calculations[8,9] predict a maximum contribution from three-body forces to the cross section of 3–4 % for the FSI situation measured. Therefore this experiment was planned to yield a statistical accuracy of the cross section data well below this level, thus providing also for a reasonably small absolute error of the analyzing power.

II. EXPERIMENT

The $^2H(\vec{p},pp)n$ reaction was measured with polarized protons from the Lamb-shift polarized ion source LASCO (Ref. 10) and accelerated to 14.1 MeV by the HVEC FN tandem Van de Graaff accelerator of the University of Köln. The beam current from the source was 200—400 nA and on target 100—200 nA, the beam polarization showed long-term variations between $P_y=0.60$ and 0.76 (± 0.03). The polarization direction was perpendicular to the reaction plane and was switched periodically between up and down in order to reduce experimental asymmetries.

The target was a foil of deuterated polyethylene with a thickness of about 100 $\mu g/cm^2$ with layers of 10 $\mu g/cm^2$ of carbon evaporated onto both sides for better thermal stability. The decrease of the deuterium content by beam evaporation could be limited to about 13% in 10 h at a beam current of 100 nA by rotating the target at about 1000 turns/minute.

The reaction products were registered by Si surface barrier detectors, most of them cooled to below -20 °C. Their solid angles were 1.07 ± 0.01 msr and they were mounted at a distance of 260 mm from the target in an ORTEC 2800 scattering chamber. The experiment was kinematically complete, i.e., the two outgoing protons were measured in coincidence in the reaction plane on either side of the beam. The collinear and the FSI situation were measured simultaneously with one detector at $\theta_3=52.6°$, $\phi_3=0°$, the other at $\theta_4=60.5°$, $\phi_4=180°$ (approximate collinearity), and $\theta_4=40.5°$, $\phi_4=180°$ (FSI), respectively. The collinearity could only be approximate due to the construction of the scattering chamber. At the angles chosen, $E_{c.m.}$ of the neutron is not exactly zero but has a minimum value of 0.5 keV which changes the collinear point into a collinear region. When defining the end points of this collinear region by the condition, that the angle θ_{4-35} between the particle 4 (one proton) and the p-n subsystem be minimal, this region extends from $\tau=9.4$ to 10.2 MeV. In view of the finite angular aperture of the detectors, which also leads to an extended collinearity region, this procedure seems tolerable. The collinear situation was selected such that interference from the quasifree scattering process was minimal; here the minimum neutron energy in the laboratory system assumes a value of 1.6 MeV.

The breakup cross section was normalized absolutely by comparing the elastic proton scattering from ^2H with results from the recent literature.[11] The beam polarization was obtained simultaneously with the breakup reaction measurement by measuring the elastic scattering of the protons from ^{12}C with two detectors at $\theta=160°$, $\phi=0°$ and 180°, and using the well-known analyzing power of this scattering.[12,13]

Standard fast-slow coincidence electronics was used for the measurements. The data in the form of energy and time-of-flight difference spectra as well as an E_3-E_4 energy matrix showing the kinematical curve were displayed on line and stored on magnetic tape event by event as triples (E_3, E_4, Δt) for off-line data reduction. The time-of-flight difference between the coincident protons was used to discriminate against the accidental background and reaction products from competing coincident two-particle and breakup reactions.

Figure 1 shows the time-of-flight difference spectrum of the collinear measurement as an example. It displays a nearly constant background and two well-separated peaks, one from the three-particle breakup, the other from a two-particle coincidence of the reaction $^{12}C(p,p)^{12}C$. The background subtraction is done by setting a window in this spectrum around the three-particle peak and a second window in the region of the purely accidental events which is chosen as wide as possible. In order to obtain the true events the background, weighted with the ratio of the two window widths, is subtracted from the measured events. Figure 2 demonstrates the effect of this background reduction on the (E_3-E_4) energy matrix for one measurement of the collinear case. Whereas in the upper part of the figure the events on the kinematical curve are obscured by two-particle reactions, they show up clearly in the lower part, i.e., after background subtraction.

An additional procedure is possible if unwanted three-particle and/or two-particle coincidences cannot be eliminated either in the two-dimensional energy spectrum or in the time-of-flight difference spectrum. Here a "time matrix" is calculated by plotting the experimental time-of-flight difference against the time-of-flight difference calculated for all reactions with the masses and energies of the three-particle reaction investigated. In this matrix different reactions cover different regions which allows for a good separation of different reactions. This can be used for particle identification instead of using detector telescopes. In our case, however, this proved to be unnecessary. The method was applied nevertheless because it has the additional advantage to reduce the statistical errors of the final data by reducing the time window width for the true events when projecting the selected events in the time matrix along a suitable direction.

Both methods together provide for a practically complete background reduction. This is illustrated by Fig. 3

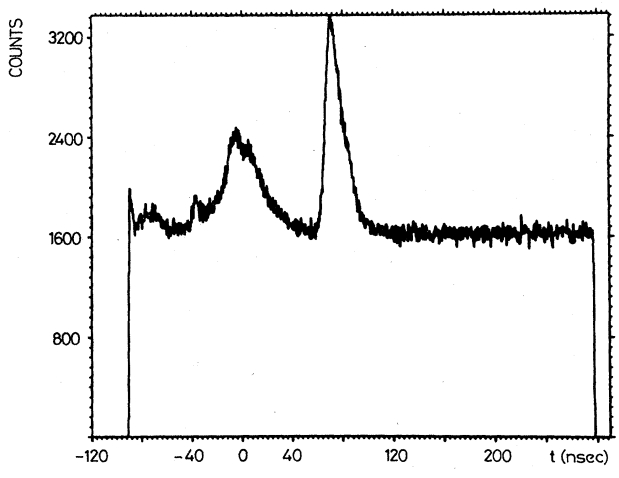

FIG. 1. Time-of-flight difference spectrum for one measurement in the collinear case. The left prominent peak is from the three-particle coincidence.

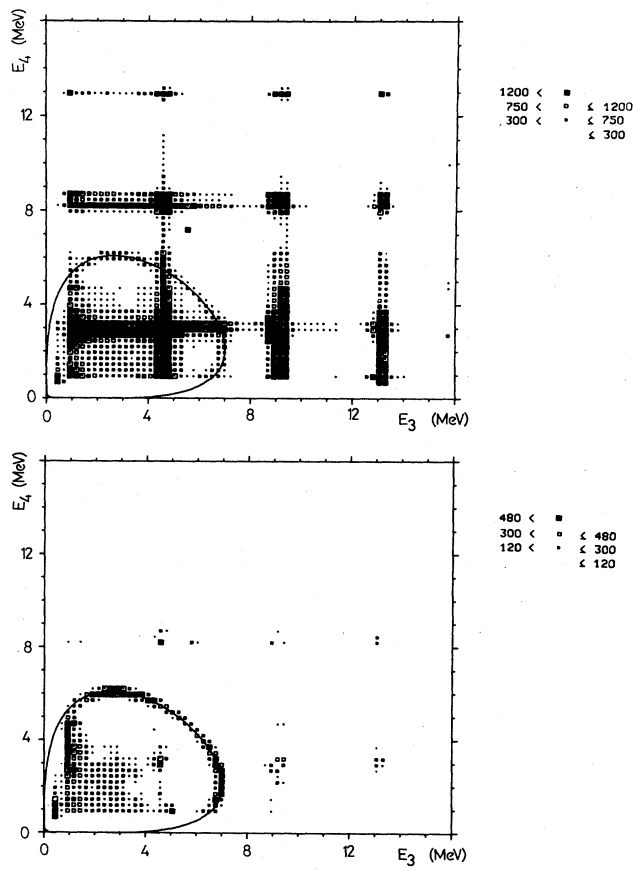

FIG. 2. (E_3-E_4) energy matrix of one measurement for the collinear case with (bottom) and without (top) background reduction. The solid line is the theoretical kinematical curve which was calculated from energy and momentum conservation.

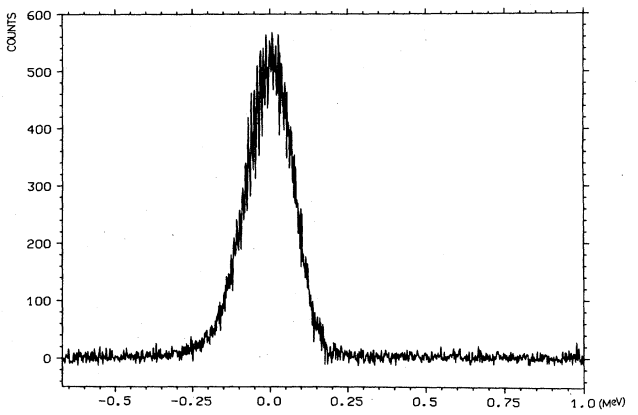

FIG. 3. Distribution of all true events around the kinematical curve, summed up along this curve, for one measurement of the FSI case. It is plotted as a function of the distance (in MeV) from the theoretical kinematical curve in the E_3-E_4 plane. 0 MeV designates the location of this curve.

in which the distribution of all true events around the calculated kinematical curve as a function of the distance from this curve in the E_3-E_4 plane, summed over the entire arc length, is plotted. The peak with a width of about 500 keV contains only true events which then were projected onto the kinematical curve. For that purpose the curve in the momentum plane, which is an ellipse, was divided into sectors corresponding to equal angular intervals $\Delta\omega$ with respect to its center. The true events contained in each sector were then projected onto the corresponding segment of the curve. The relation between the angular parameter and the energies E_3,E_4 is given by

$$\omega=\arctan(T_3 b/T_4 a),\quad 0\le\omega\le 2\pi\ ,$$

with

$$\begin{bmatrix}T_3\\T_4\end{bmatrix}=\left[\begin{bmatrix}\sqrt{E_3}\\\sqrt{E_4}\end{bmatrix}-\begin{bmatrix}x_3\\x_4\end{bmatrix}\right]\begin{bmatrix}\cos\alpha & \sin\alpha\\-\sin\alpha & \cos\alpha\end{bmatrix}$$

and (x_3,x_4): ellipse center; a,b: major and minor semiaxes of the ellipse; and α: angle between a and the $\sqrt{E_3}$ axis. The cross section and the analyzing power are thus obtained as a function of the angular parameter ω. For a comparison with theoretical calculations these data had to be transformed into functions of the arc length parameter τ in the energy plane. Because constant angular intervals $\Delta\omega$ do not correspond to constant arc length intervals of the ellipse, this transformation leads to varying arc length intervals $\Delta\tau$ in the energy plane. Our results are presented with the arc length parameter τ running clockwise with $\tau=0$ being arbitrarily identified with the minimum value of E_3 and the larger of the possible two values of E_4.

III. THEORETICAL CALCULATIONS

The Faddeev calculations for this comparison were of two types. Stuivenberg's code SASA 3 (Ref. 14) from 1976 was run in Bochum and Doleschall performed calculations with his 1983 code.[15,16] Both codes are based on the Alt-Grassberger-Sandhas formulation of the Faddeev equations;[17] they use separable potentials and take into account the Coulomb effect only perturbatively. The code by Stuivenberg uses only S waves and therefore cannot predict any vector analyzing powers. His form factors are of the rank-two Yamaguchi-type:

$$g_S(p)=\frac{\gamma_S}{(\beta_S^2+p^2)}\ ,$$

where S is the channel spin.

Doleschall's code takes into account P and D wave interactions in addition to S waves and a tensor force. For each of these interactions a form factor of rank five of the "realistic-type" was used

$$g_{i(LS)J}(p)=\frac{p^L}{(1+\beta_{iL}p^2)^L}\sum_{k=1}^{5}\alpha_{kiL}\left[\frac{1}{1+\beta_{iL}p^2}\right]^k .$$

The potential contained the following terms:[16]

(a) three-term singlet S-wave interaction $^1S_0$;

(b) two-term triplet P-wave interaction $^3P_0$;

(c) one-term $^1P_1$, $^3P_1$, $^3P_2$, $^1D_2$, $^3D_2$, and $^3D_3$ interactions;

(d) four-term tensor force $^3S_1$-$^3D_1$ with a deuteron D-state probability of 4% (deuteron quadrupole moment $Q=0.286$ fm^2, asymptotic D/S ratio $A_D/A_S=0.0272$).

The potential used reproduces the NN phase shifts up to 400—500 MeV. Table I shows the low-energy and bound-state data of the two sets of potential parameters.[16,18]

IV. RESULTS AND DISCUSSION

Figures 4—7 show the experimental results. The absolute differential cross sections were obtained from the expression

$$\frac{d^3\sigma}{d\Omega_3 d\Omega_4 d\tau}\{\xi\}=\left\langle \frac{N\{\xi\}}{G_{\text{coinc}}}\frac{G_{\text{mon}}}{N_{\text{mon}}}\left[\frac{d\sigma}{d\Omega}(\theta_{\text{mon}})\right]_{\text{elastic}}\right\rangle .$$

Here $\{\xi\}=\{\theta_3,\phi_3,\theta_4,\phi_4,\tau,E_p\}$ is the set of parameters which fully characterizes the variables of the kinematically complete three-particle experiment, G_{coinc} and G_{mon} are the geometrical factors of the two detectors in coincidence and of the monitor detector, $N\{\xi\}$ and N_{mon} are the coincident and monitor detector yields, respectively, and $[d\sigma/d\Omega(\theta_{\text{mon}})]_{\text{elastic}}$ is the known laboratory elastic scattering cross section. The average was taken over spin up and down runs with a polarized beam.

The analyzing powers obtained from the expression

$$A_y\{\xi\}=\frac{N^{\uparrow}\{\xi\}-N^{\downarrow}\{\xi\}}{N^{\uparrow}\{\xi\}+N^{\downarrow}\{\xi\}}P_y^{-1}$$

are plotted along the kinematical curve, i.e., as a function of the arc parameter τ, both for the collinear and the FSI case. In the collinear case the collinear region is located around the arc parameter value of $\tau=9.8$ MeV. The solid curves in Figs. 4(a) and (b) and 5(a) and (b) are the results of Faddeev calculations by Doleschall, whereas the curves in Figs. 6 and 7 are predictions from calculations with the Stuivenberg code.

TABLE I. Scattering lengths, effective ranges, and deuteron binding energy from potential sets of Faddeev calculations used in this work.

		Stuivenberg (Ref. 18)	Doleschall (Ref. 16)
Singlet $^1S_0$:	a_{pp} (fm)	−7.82	
	a_{nn} (fm)		−16.99
	a_{np} (fm)	−23.78	−23.63
	r_{nn} (fm)	2.83	2.84
	r_{np} (fm)	2.67	2.50
Triplet $^3S_1$:	a_{np} (fm)	5.41	5.41
	r_{np} (fm)	1.76	1.76
Deuteron binding energy:	ϵ_d (MeV)	2.226	2.225

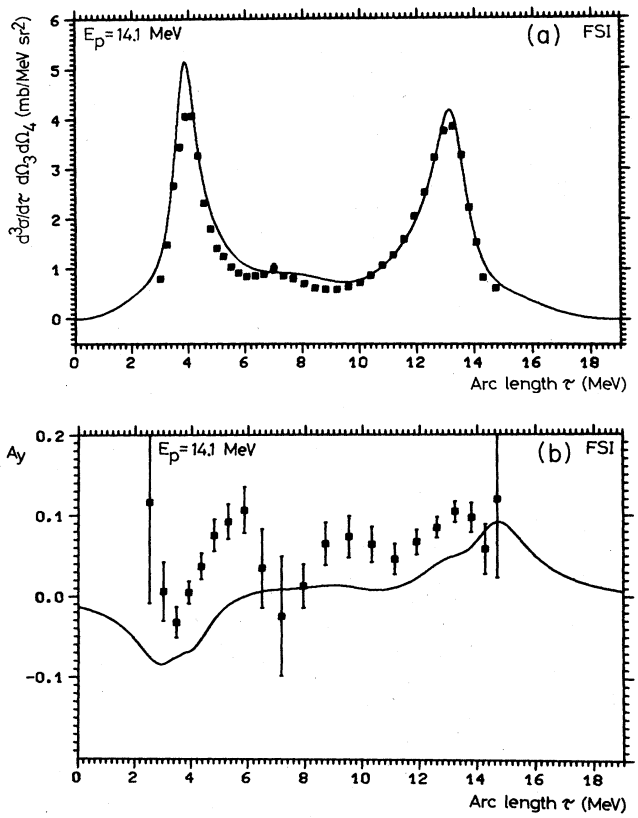

FIG. 4(a) and (b). Differential cross section (a) and analyzing power (b) as a function of the arc parameter τ for the FSI situation with $\theta_3=52.6°$, $\phi_3=0°$, $\theta_4=40.5°$, and $\phi_4=180°$. The solid lines are the predictions by Doleschall (Ref. 16).

A. Differential cross section

The differential cross section was determined with an overall error of 2—3 % combined quadratically from statistical errors, errors of the elastic cross section, and errors of the geometrical factors of the detectors. The agreement between the data and both types of Faddeev calculations is quite satisfactory. The FSI peaks are well reproduced and for the region between the peaks the calculations predict slightly higher values. The calculation by Doleschall, however, reproduces this region slightly better as can be expected due to the much more sophisticated potential used. The indication of a small peak in this region is the result of the incomplete subtraction of a two-particle coincidence.

In the collinear case the differences between the two types of Faddeev calculations are larger. The shape of the spectrum is well reproduced by both, but the absolute magnitude is underestimated by Stuivenberg's code especially in the region between the peaks, whereas the calculation by Doleschall is quite satisfactory.

B. Analyzing power

The magnitude of the measured analyzing power is below 0.1 for the collinear as well as for the FSI case.

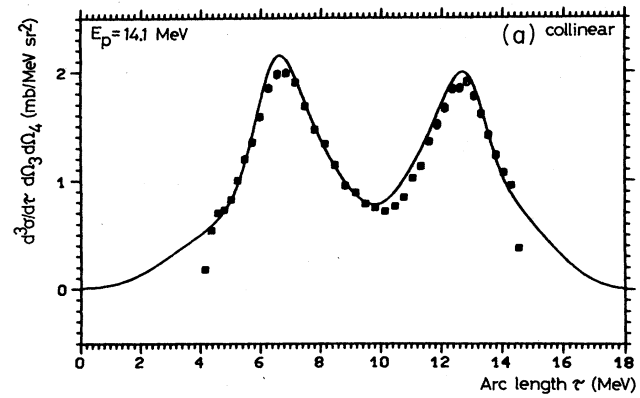

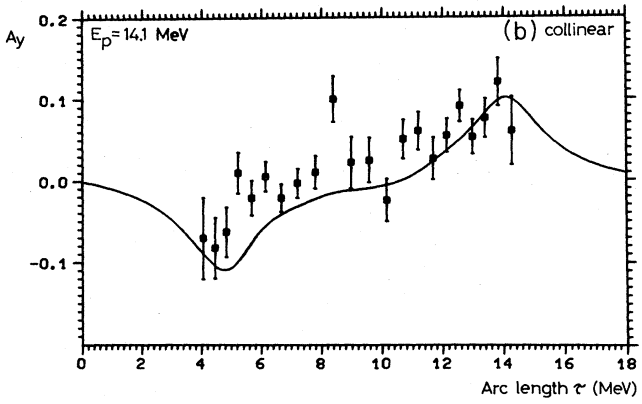

FIGS. 5(a) and (b). Differential cross section (a) and analyzing power (b) as a function of the arc parameter τ for the (approximately) collinear situation with $\theta_3=52.6°$, $\phi_3=0°$, $\theta_4=60.5°$, and $\phi_4=180°$. The collinear point is at $\tau=9.8$ MeV, the collinear region, as defined in the text, reaches from $\tau=9.4$ to 10.2 MeV. The solid lines are the predictions by Doleschall (Ref. 16).

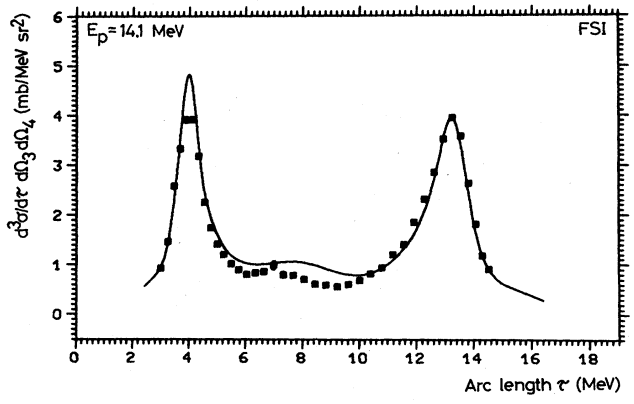

FIG. 6. Differential cross section as a function of the arc parameter τ for the FSI situation together with the prediction from calculations with the code by Stuivenberg (Ref. 18) (solid line).

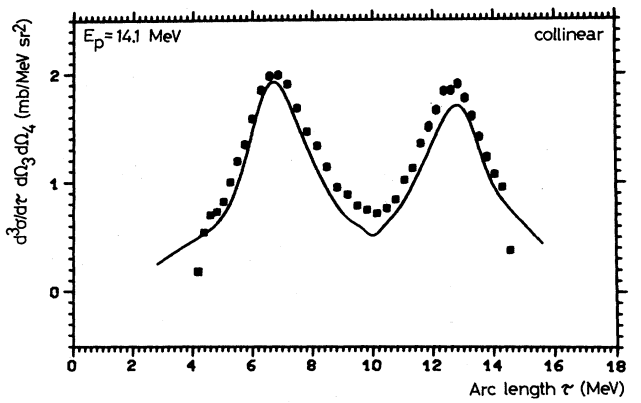

FIG. 7. Differential cross section as a function of the arc parameter τ for the (approximately) collinear situation together with the prediction from calculations with the code by Stuivenberg (Ref. 18) (solid line).

The error of most data points is around 0.02. The analyzing power seems to have more structure than the cross section. The calculation by Doleschall agrees with the data in the maximum value of 0.09 of the magnitude of the analyzing power, but the dependence on the arc parameter τ is reproduced only coarsely. Especially in the FSI case, the comparison is not satisfactory since the theoretical analyzing power is 0.03—0.06 below the measured one in a region where the error is only 0.02.

V. SUMMARY

Both types of Faddeev calculations with the codes by Stuivenberg and by Doleschall are able to reproduce the cross section data without any relative adjustment of either. The results of Doleschall prove to be superior in detail. This is true especially for the region between the FSI peaks in the collinear and also in the pure FSI situation, where due to the lack of dominant reaction mechanisms it seems important to use more complicated potentials including higher waves and a tensor force.

The analyzing power is not reproduced well and therefore appears, as expected, to be a more sensitive observable than the cross section, and therefore also a more critical quantity to distinguish between potentials in Faddeev calculations. The behavior of the analyzing power in the FSI case suggests a search for modified parameter sets in Faddeev calculations. On the experimental side measurements of polarization observables even in three-particle breakup reactions appear mandatory for future work on the NN interaction, but with still higher accuracy.

As expected from the recent Bochum calculations including a three-body force,[8,9] no additional structure such as a peak is visible in the data. The calculation by Doleschall, i.e., without a three-body force is even able to reproduce quite well the data in the sensitive region where the Bochum calculations (which are not depicted in this work) predict an increase of the cross section by the three-body force. The data in this region are rather slightly below the values calculated by Doleschall. Any contribution from three-body forces must therefore be small,

i.e., of the order of the error or smaller. An upper limit for this contribution in our case for the most sensitive region is thus 2—3 % of the two-body cross section.

On the other hand the calculations with Stuivenberg's code predict a cross section too small by about 15% as compared with the data which would satisfy the prediction of Refs. 8 and 9, but the comparison with Doleschall's results shows that this is due to the neglect of higher waves and certainly not to three-body forces (see also Ref. 7).

Since phase space regions without dominant reaction mechanisms are most promising to search for three-body force effects and these regions are also more sensitive to higher contributions such as P and D waves and the tensor force, only "advanced" Faddeev codes should be supplemented by three-body potential terms.

The analyzing power also gives no hint to the existence of three-body force effects. Nevertheless the question of spin dependence of the three-body force remains open and should be investigated theoretically.

ACKNOWLEDGMENTS

The authors are grateful to Dr. P. Doleschall for performing the calculations with his code for them and also to Dr. W. Meier and P. Lekkas for the calculations with the Stuivenberg code. They thank them and Dr. W. Glöckle, Dr. R. Brandenburg, and Dr. J. Zabolitzky for helpful discussions. This research was in part supported by the Bundesministerium für Forschung und Technologie, Bonn, Federal Republic of Germany.

[1]F. Foroughi, Ch. Nussbaum, H. Vuilleumier, and B. Vuilleumier, Nucl. Phys. **A346**, 139 (1980).

[2]F. D. Correll, G. G. Ohlsen, R. E. Brown, R. A. Hardekopf, N. Jarmie, and P. Doleschall, Phys. Rev. C **23**, 960 (1981).

[3]P. Doleschall, Nucl. Phys. **A201**, 264 (1973); **A220**, 491 (1974); P. Doleschall, Uppsala Tandem Accelerator Laboratory Report TLU-58/78, 1978.

[4]R. Brandenburg and W. Glöckle, Nucl. Phys. **A377**, 379 (1982).

[5]H. T. Coelho, T. K. Das, M. R. Robilotta, and M. Isidro Filho, *Tenth International IUPAP Conference on Few Body Problems in Physics, Karlsruhe, 1983,* edited by B. Zeitnitz (North-Holland, Amsterdam, 1984), Vol. II, p. 497.

[6]W. Meier and W. Glöckle, Phys. Rev. C **28**, 1807 (1983).

[7]J. Birchall, J. P. Svenne, M. S. de Jong, J. S. C. McKee, W. D. Ramsay, M. S. A. L. Al-Ghazi, and N. Videla, Phys. Rev. C **20**, 1585 (1979), and references therein.

[8]W. Meier, private communication.

[9]A. Bömelburg, W. Glöckle, and W. Meier, *Tenth International IUPAP Conference on Few Body Problems in Physics, Karlsruhe, 1983,* edited by B. Zeitnitz (North-Holland, Amsterdam, 1984), Vol. II, p. 483.

[10]V. Bechtold, L. Friedrich, P. Ziegler, R. Aniol, G. Latzel, and H. Paetz gen. Schieck, Nucl. Instrum. Methods **150**, 407 (1978).

[11]W. Grüebler, V. König, P. A. Schmelzbach, F. Sperisen, B. Jenny, and R. E. White, Nucl. Phys. **A398**, 445 (1983); and private communication.

[12]J. S. Dunham, M. P. Baker, J. G. Cramer, H. O. Meyer, T. A. Trainor, and W. G. Weitkamp, University of Washington, Nuclear Physics Laboratory Annual Report, 1975.

[13]G. Latzel and H. Paetz gen. Schieck, Nucl. Phys. **A323**, 413 (1978).

[14]Code SASA III by J. H. Stuivenberg, Information on the computer codes of Dr. Bruinsma, University of Tübingen, 1976; W. Meier and P. Lekkas, private communication.

[15]P. Doleschall, W. Grüebler, V. König, P. A. Schmelzbach, F. Sperisen, and B. Jenny, Nucl. Phys. **A380**, 72 (1982).

[16]P. Doleschall, private communication.

[17]E. O. Alt, P. Grassberger, and W. Sandhas, Nucl. Phys. **B2**, 167 (1967).

[18]P. Lekkas, private communication.